Advanced Ceramics Progress: Vol. 9, No. 2, (Spring 2023) 8-15

Materials and Energy Research Center
MERC

Contents lists available at ACERP

Advanced Ceramics Progress

Journal Homepage: www.acerp.ir

Original Research Article

Characterization of Flowability and Compaction Behavior of Biomedical Ti-Cu Intermetallic Alloy Synthesized by Mechanical Alloying Method

Mohammad Reza Akbarpour [a,*], Solmaz Moniri Javadhesari [b]

[a] *Professor, Department of Materials Engineering, Faculty of Engineering, University of Maragheh, Maragheh, P.O. Box 83111-55181, Iran*
[b] *Assistant Professor, Department of Biology, Faculty of Basic Sciences, Azarbaijan Shahid Madani University, Tabriz, Iran*

* Corresponding Author Email: akbarpour@maragheh.ac.ir (M. R. Akbarpour)

URL: https://www.acerp.ir/article_169262.html

ARTICLE INFO

Article History:

Received 25 February 2023
Received in revised form 27 March 2023
Accepted 5 April 2023

Keywords:

Mechanical Alloying
Flowability
Compressability
Ti-Cu Alloy

ABSTRACT

This study investigated the flowability and compactability of the milled Ti-Cu alloys as a new version of biomedical alloys used for fabrication via Additive Manufacturing. In this study, Ti- 50 at. % Cu powder was first milled for different durations, and the morphology, microhardness, size, flowability, and compactability of the powder were assessed. The results indicated that while flowability increased with prolonged milling time, compressibility decreased owing to a decrease in the plastic deformation capacity. The highest flowability level was obtained when hard TiCu phase was synthesized after 30 hours of milling. Different linear and nonlinear compaction equations were used to investigate the densification response of TiCu powder in a rigid mold during uniaxial compression. Cooper-Eaton nonlinear equation was found to be the best fit compared to the linear equation. The contribution of particle rearrangement to the densification behavior was high, and it increased upon increasing the applied pressure. At pressures below 1200 MPa, the contribution of plastic deformation to the powder densification was negligible.

https://doi.org/10.30501/acp.2023.387236.1118

1. INTRODUCTION

Commercially pure titanium is widely used in several dental products because of its excellent biocompatibility, corrosion resistance, and lightweight properties. However, pure Ti has some drawbacks in structural and biomedical applications such as its poor tribological and antibacterial properties, to name a few [1]. It has been reported that in dental prostheses, there is significant wear of the cast commercially pure (CP) titanium. Bacteria can also grow on Ti when bacterial infection occurs [2]. One way to solve these problems is to alloy titanium with other elements such as Cu. Alloying Ti and Cu can improve the mechanical properties required for dental applications [3]. C. Ohkubo et al. investigated the effect of alloying elements, such as Cu, on the wear resistance of Ti. They demonstrated that addition of Cu (5 wt. %) introduced Ti/Ti_2Cu eutectoid and improved the wear resistance [4]. The tribological behavior of Ti-Cu intermetallic alloys produced by Powder Metallurgy (PM) method was studied [5]. Intermetallic Ti-Cu alloys are characterized by higher wear resistance to a tungsten carbide (WC) counterface and lower friction coefficients than commercially pure titanium, and their tribological properties can be significantly enhanced upon increasing the milling time owing to the grain

Please cite this article as: Akbarpour, M. R., Moniri Javadhesari, S., "Characterization of Flowability and Compaction Behavior of Biomedical Ti-Cu Intermetallic Alloy Synthesized by Mechanical Alloying Method", ***Advanced Ceramics Progress***, Vol. 9, No. 2, (2023), 8-15. https://doi.org/10.30501/acp.2023.387236.1118

refinement and increase in the Ti_2Cu_3 content. Much research has been done so far to evaluate the antibacterial and biocompatibility of TiCu alloys [6-9]. The properties of this alloy depend on the Cu content and formed intermetallic phases. Based on the conducted research, the superior antibacterial activity and biocompatibility of the Ti-Cu alloy make it feasible to use it as an implant material with minimal bacterial infection. It is also possible to obtain antimicrobial properties in the Ti-Cu alloys by adding copper elements. The antimicrobial properties of copper make it effective in killing bacteria quickly when released into the body. Bacteria cells produce copper toxin due to the presence of Cu (I) ions that can damage cell membranes and kill bacteria.

PM [5,7], casting [1], and Selective Laser Melting (SLM) [10,11] methods have recently been widely used to produce bulk Ti-Cu alloys. The properties of the Ti-Cu alloy parts processed with PM and SLM are strongly influenced by those of the powder. Mechanical alloying with a high-energy ball mill is a manufacturing process for nanocrystalline Ti-Cu powder that has been referred to many times in the literature [12,13]. More details of the microstructural and morphological changes in Ti-Cu powder during mechanical milling can be found in previous studies [13]. As the milling time has been shown to affect the powder properties, varying process conditions such as milling time can affect the flowability and compressibility of the powder used to manufacture Ti-Cu alloy. In the literature, no studies have been conducted on the effects of Ti-Cu alloy milling time/powder features on its flowability and compactibility, which play a key role in powder densification. Therefore, in the present work, Ti-Cu powder was mechanically alloyed for different times, and its morphology, hardness, size, flowability, and compaction behavior were studied for use in processing the Ti-Cu parts.

2. MATERIALS AND METHODS

Table 1 lists the raw materials and their characteristics. A mixture of Ti–50 at. % Cu powder was ball milled in a planetary ball mill (Retsch 400MA) for different times. The milling conditions and phase transformations that occur during milling have been previously reported in several studies [13].

TABLE 1. The used raw materials and their characteristics

Material	Average Particle Size (D_{50}) (μm)	Purity (%)	Manufacturer
Ti powder	45.9	99.5	Merck, Germany
Cu powder	12.5	99.7	Merck, Germany

To investigate the microstructure of the milled powder, Scanning Electron Microscopes (SEMs, Philips XL30) equipped with EDS and Transmission Electron Microscopes (TEMs, FEG Philips CM200) with Cu Kα radiation (λ=0.154 nm) and a 0.02 degree/sec scan rate were used. As observed in the X-ray diffraction (XRD) patterns, the crystallite size and microstrain of the specimens were calculated using the Williamson-Hall method. Apparent Density (AD) and Tap Density (TD) of the powders were measured using the standard cup and funnel methods (ISO 3923). The powders milled for 1, 5, 10, 20 , 30, and 40 hours were each compressed at 400, 600, 800, 1000, 1200, and 1400 MPa, respectively, with zinc stearate acting as a die lubricant. A density measurement was performed using Archimedes' law on the green samples. Each sample was measured three times, and their mean values were reported to ensure accuracy. As part of the flowability testing, an open-base Angle of Response (AOR) method was used to measure flowability. Each AOR test utilized a funnel to pour powder onto a large horizontal plate until a cone-shaped pile of powder formed, grew to a sufficient height, and no more powder accumulated. A digital camera was used to image the pile, and the angle value was measured by image analysis.

3. RESULTS AND DISCUSSION

3.1. Changes in the Structure and Morphology

The Ti-Cu powder was mechanically milled for different times using high-energy ball milling. At the beginning of milling, only severe plastic deformation occurred under the steel ball impact. Figures 1a and 1b demonstrate the flakes of Ti and Cu powder mixture milled for five hours. As the milling progressed, the strong impact of the steel ball made the particles of the powder mixture plastically deformed that led to the formation of a cold weld, revealing a prominent lamellar structure. With further milling, the distance between the lamellae decreased. As shown in Figures 1c and 1d, no lamellar structures can be observed after 30 hours of milling. At this stage, the microstructure of the powder was uniform. Our previous work described the morphological and microstructural changes in the Ti-Cu powder during milling. The average particle size after different milling times was measured using SEM micrographs, the values of which are listed in Table 2. The change in the Ti-Cu powder particle size with milling time showed an identical tendency to that of metal powders in general. During the first hours of milling, when cold welding is the dominant mechanism, the average particle size increases. When the milling is prolonged, work hardening results in the fracture of milled powders and the reduction of the particle size. After milling for a certain length of time, steady-state

equilibrium is obtained when a balance is achieved between the rate of welding, which tends to increase the average particle size and rate of fracturing, thus leading to a decrease in the average particle size.

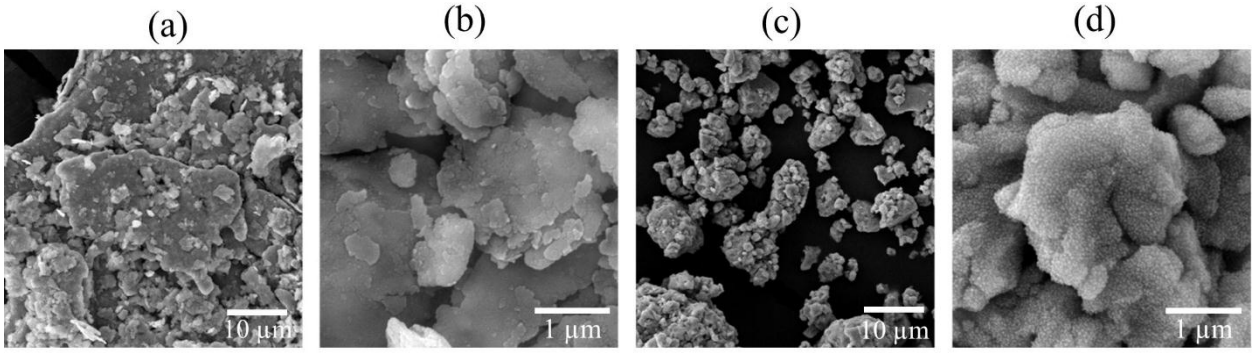

Figure 1. SEM micrographs illustrating the morphology of Ti-50 at. % Cu powder alloyed for 5 h (a, b) and 30 h (c, d)

TABLE 2. Features of the powder milled for different times

	Milling Time, h					
	1	5	10	20	30	40
Average Particle Size, µm	15.3	23.4	37.8	28.2	25.9	24.0
Grain Size, nm	98	35	29	17	7	6
Powder Morphology	Flake	Flake	Flake	Small Flake/Equiaxed	Equiaxed	Equiaxed
Phases	Ti, Cu	Ti, Cu	Ti, Cu	Ti, Cu	TiCu	TiCu

The Ti-Cu intermetallic powder was synthesized by milling Ti-Cu powder mixtures for 30 h. Table 2 summarizes the phases and crystallite sizes obtained from the XRD results of the powders milled for different times. The powder flow and compaction behaviour were explained based on these data.

Figure 2 depicts the SEM image of the powder particles mechanically alloyed for an hour as well as the maps of Ti and Cu distributions on the surfaces of the particles. As shown in this figure, Ti and Cu are not evenly distributed on the powder particles. Some regions of the microstructure were rich in Ti while others were rich in Cu (Figures 2a, 2b, and 2c).

Based on the EDS analysis (Figure 2d), sharp peaks are associated with major Ti while the faint ones are associated with minor Cu. Work hardening and fracturing of the powder gradually distributes the alloying elements into the powder volume as the MA period increases. Figure 3 shows the elemental maps of the distribution of Ti and Cu in the SEM image of the powder particles after 30 hours of milling. This figure also confirms that the alloying elements are evenly dispersed in the powder (Figures 3b and 3c). The EDS analysis (Figure 3d) reveals the approximately equal mol % presence of Ti and Cu in the particles, confirming their uniform dispersion at the atomic level.

3.2. Apparent and Tap Densities and Flowability

As shown in Figure 4a, the milling time affects the apparent and tap densities of Ti-50 at. % Cu powder. As the milling time increased, the apparent and tap densities decreased and then increased. Hausner Ratio (HR) represents the relationship between the powder tap and apparent densities. It also indicates the flow potential of the powder. The higher the HR value, the lower the flowability of the powder at the beginning of the compaction. The HR value greater than 1.25 is indicative of the poor powder flowability.

The relationship between the HR and milling time for the Ti-Cu powder is shown in Figure 4b. The HR variation with the milling time depicted three distinct zones, i.e., 1-10, 10-30, and more than 30 h. Milling up to 10 hours results in a high HR due to the flake shape of the powders. During the first few hours of milling, the powders undergo plastic deformation and cold-welding, and they take a layered shape with poor flowability. Milling the powder for more than 10 hours induces work hardening and fracture in addition to plastic deformation. This in turn reduced the relative size of the powder and increased their sphericity. A milling process lasting more than 30 hours has little effect on the particle size and morphology of the powder and thus on the HR of the product. As shown in Figure 5, the AOR varied with the milling time. As the AOR increased, there was a stronger force between the particles, which reduced the flowability of the powder. AOR increased when the powder was mechanically milled for up to 10 hours. This increase was associated with the flake morphology of the

powder as well as the increase in the flake size. Based on the figure, it is evident that milling for longer than 10 minutes reduced the AOR, and milling for 30 minutes yielded the lowest AOR, indicating the highest flowability. This is related to the changes in the powder morphology from flaky to equiaxial, which occur during milling.

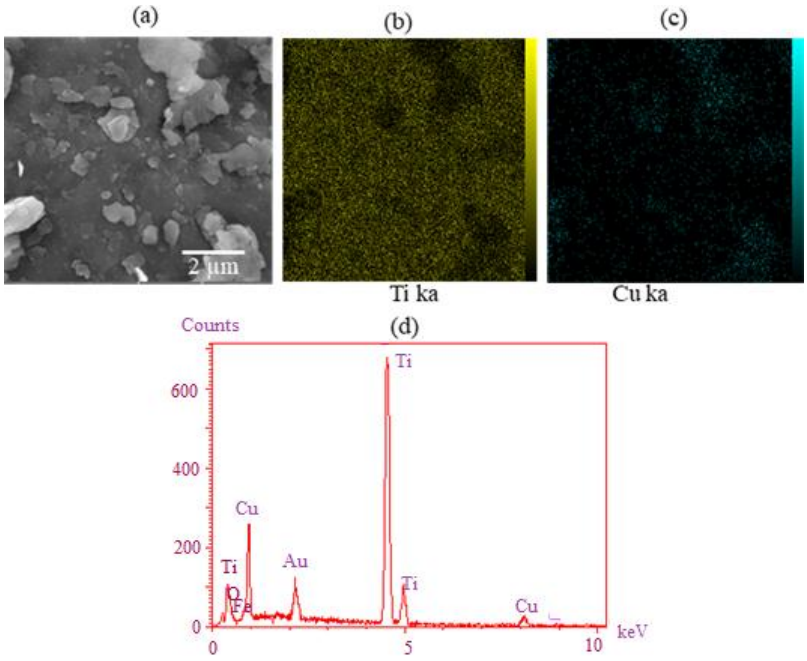

Figure 2. (a) SEM micrograph of a particle surface, (b) Ti distribution, (c) Cu distribution, and (d) EDS analysis of the 1 h mechanically alloyed Ti–Cu powder

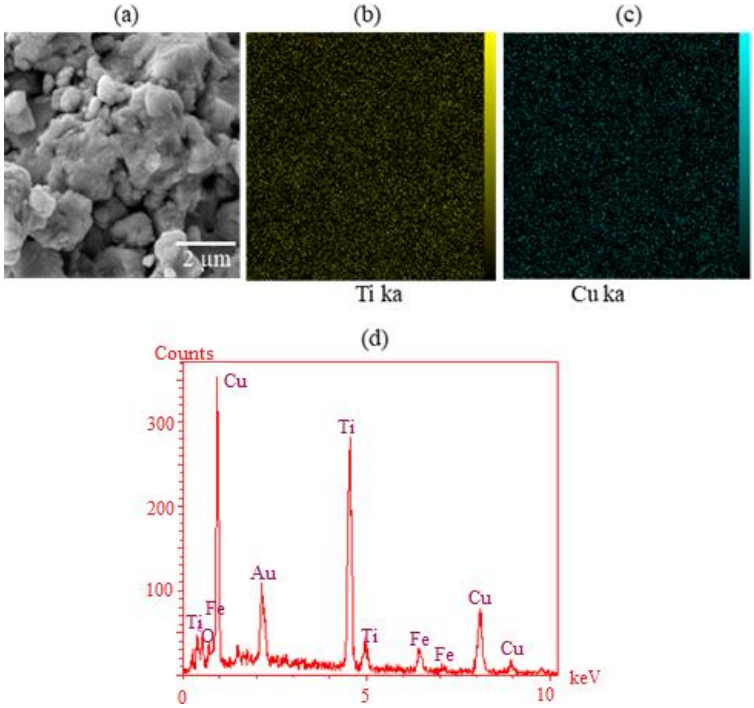

Figure 3. (a) SEM micrograph of a particle surface; (b) Ti distribution; (c) Cu distribution; and (d) EDS analysis of the 30 h mechanically alloyed Ti–Cu powder

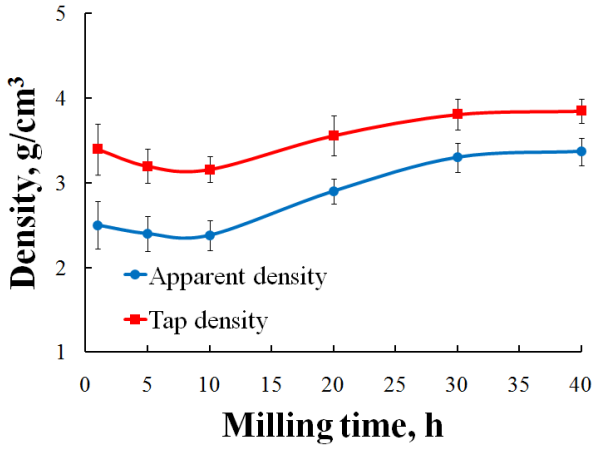

(a)

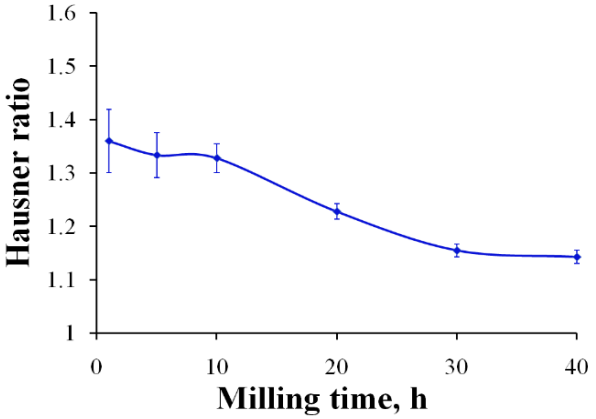

(b)

Figure 4. (a) TD and AD versus MM time, and (b) HR versus MM for Ti-50 at. % Cu powder

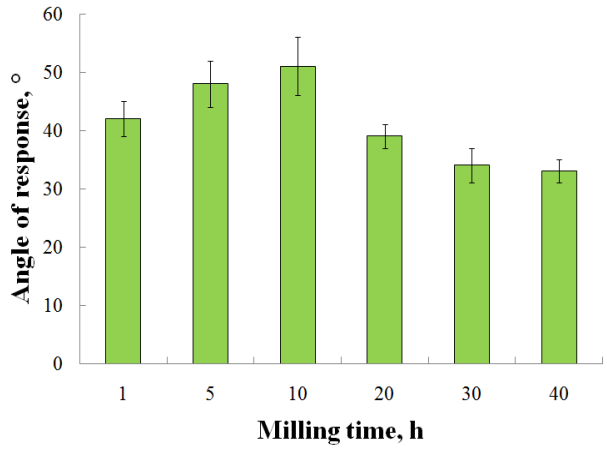

Figure 5. The angle of repose of the alloy powder milled for different times

To assess the variations in the density of the green samples with the milling time, the powders milled for different durations were compacted at 600 MPa. Figure 6 depicts the relationship between the compact density and milling time. Although the flowability of the powder increases with the milling time owing to work hardening and formation of a hard TiCu phase, the plastic deformation capacity of the powder during compression diminishes, resulting in a decrease in density. Owing to the hardening effect of mechanical milling, the green density of the compacts tends to decrease upon increasing milling duration for the metallic powders. In Figure 6, plastic deformation was found to be important for determining the green density of a powder. In terms of green density, powders with excellent plastic deformation properties (with a shorter milling time) showed the highest values.

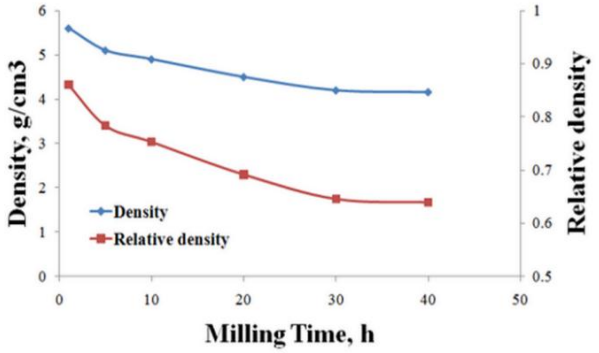

Figure 6. Variations in the density of green samples compressed at 600 MPa pressure with milling time

3.3. Compressibility of TiCu powder

Figure 7 depicts the compressibility curve of the TiCu powder milled for 30 hours and compacted under various pressures. The Ti-Cu powder milled for 30 hours has an intermetallic TiCu structure and high hardness. As the applied pressure increased, the relative density increased as well. The densification of metallic powders under pressure is a two-stage process that includes Particle Rearrangement (PR) at low pressure and Plastic Deformation (PD) at high pressures. These mechanisms are usually active simultaneously, particularly at the local scale. The hardness of the TiCu powder was 634 HV. As a result, particle rearrangement plays a major role in densification at low pressures. Linear modified Heckel, Panelli-Filho, and Ge equations as well as non-linear Cooper and Eaton equations [14-17] were used to assess the data compressibility. The Equations are as follows:

$$\text{Heckel: } \ln(1/(1-D)) = K_1 P + B_1 \quad (1)$$

$$\text{Panelli-Filho: } \ln(1/(1-D)) = K_2 \sqrt{P} + B_2 \quad (2)$$

$$\text{Ge: } \log[\ln(1/(1-D))] = K_3 \log(P) + B_3 \quad (3)$$

Cooper and Eaton:

$$(1/D_0-1/D)/(1/D_0-1) = A_1 \exp(C_1/P)+A_2 \exp(C_2/P) \quad (4)$$

where D_0, P, and D represent the initial relative density of the powder, applied pressure, and relative density under the applied pressure, respectively. The densification indexes K_1, K_2, and K_3 describe the ease with which the powder can be compacted by both PR and PD under an applied load. The constants C_1 and C_2 describe the pressures at which this two-stage densification is expected to occur.

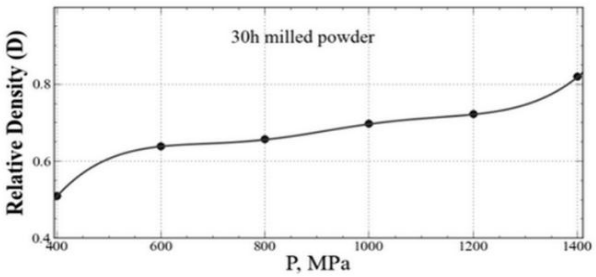

Figure 7. Compaction pressure effects on the relative density of TiCu mechanically milled for 30 h

To determine the densification behavior of the TiCu powder, the experimental data shown in Figure 7 were fitted with several linear and nonlinear equations (Figures 8 and 9). Curve Expert Professional software was utilized to carry out the statistical analysis (Version 1.6.5). Table 3 summarizes the results. The Cooper and Eaton non-linear equation fits the experimental findings for TiCu powder quite well, according to the analysis of variance with a high coefficient of determination (R2 = 0.992). The maximum coefficient of determination was obtained using the Cooper and Eaton equation. coefficients of determination of the linear equations were < 0.976.

An illustration of the roles of the PR (A_1Exp (C_1/P) and PD (A_2Exp (C_2/P) mechanisms in TiCu powder densification is shown in Figure 9. According to the figure analysis, the PR significantly contributes to densification and increases with increasing pressure. However, the PD mechanism signoficantly contributes to densification at pressures higher than 1400 MPa. According to this study, a nonlinear Cooper-Eaton equation can accurately describe the densification behaviour of TiCu powder.

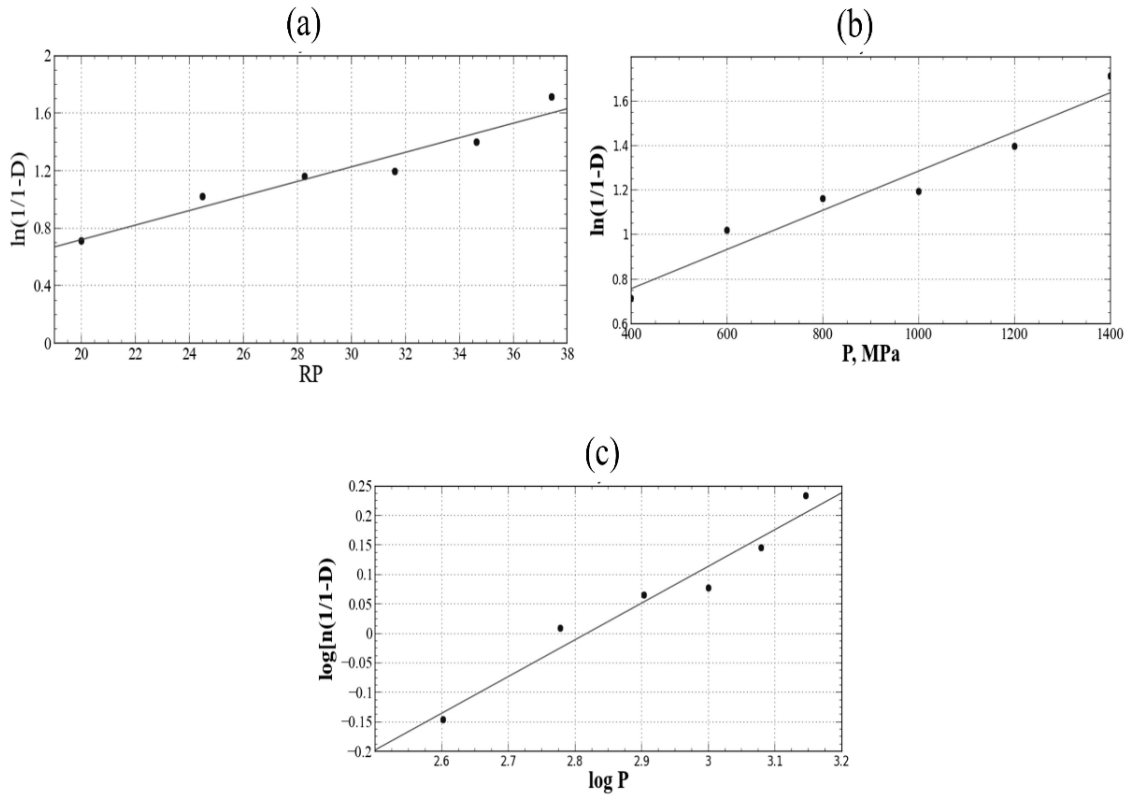

Figure 8. Experimental data of TiCu nanoctructured powder, fitted by linear modified Heckel (a) , Panelli-Filho (b), and Ge (c) equations

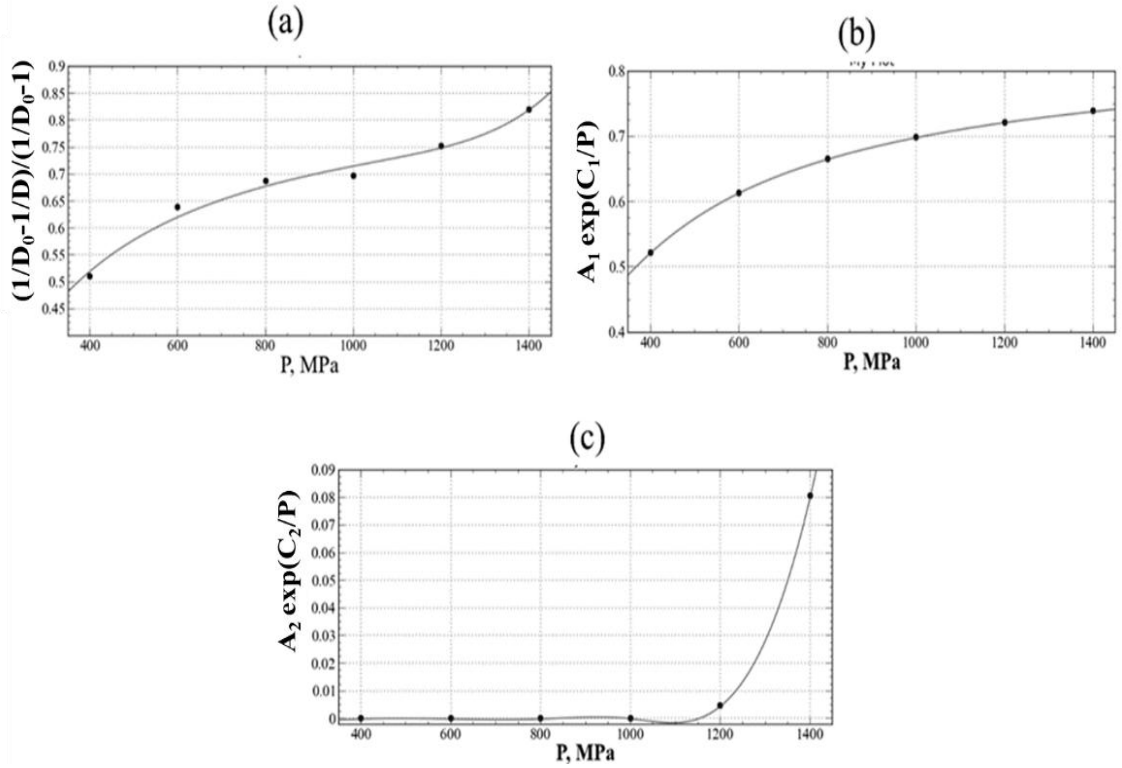

Figure 9. Experimental data of TiCu nanostructured powder, fitted by Cooper and Eaton non-linear equation (a), and the contribution of (b) particle rearrangement ($A_1Exp\ (C_1/P)$, and (c) plastic deformation ($A_2Exp\ (C_2/P)$ mechanisms on the densification of the powder

TABLE 2. An analysis of the compressibility of TiCu powder using linear compaction equations. R^2 represents the coefficient of determination and MPa^{-1} is the dimension of densification indexes

Heckel		Panelli-Filho		Ge		Cooper and Eaton non-linear equation				
K_1	R^2	K_2	R^2	K_3	R^2	A_1	A_2	C_1	C_2	R^2
0.009	97.3	0.05	96.8	0.62	97.6	6.5E+03	1.6E+04	0.88	211.1	99.2

4. CONCLUSION

The microstructural and morphological evolution, flowability, and compressibility of the Ti-50 at. % Cu powder milled for different times were investigated in this study. Followed by an increase in the milling time, the change in the powder size and morphology was similar to that of the pure metal. Increasing the milling time up to 10 hours reduced the tap and apparent densities of the alloy; however, further milling improved them. The green density of the powder mixture was reduced after milling. After milling for 10 hours, the AOR of the powder increased, indicating a greater force between the particles and a decreased flowability. Increasing the milling time from 10 to 40 hours reduced the AOR of the powder and improved the alloy flowability, thus making it suitable for consolication. The determining factor in the flowability of this powder is its morphological change from a flake to equiaxed. A mathematical model for the compressibility of metallic alloyed powders (e.g., TiCu powder) was proposed using linear and non-linear compaction equations. A comparison of the linear and non-linear equations revealed that Cooper and Eaton's non-linear equation provided the best fit. Particle rearrangement was found to play a significant role in the densification process, and this effect was intensified with pressure. Plastic deformation was negligible under the applied pressure of 1200 MPa.

ACKNOWLEDGEMENTS

The author wish to acknowledge University of Maragheh for the all support throughout this work.

REFERENCES

1. Pripanapong, P., Tachai, L., “Microstructure and mechanical

properties of sintered Ti-Cu alloys", ***Advanced Materials Research***, Vol. 93-94, (2010), 99-104. https://doi.org/10.4028/www.scientific.net/AMR.93-94.99
2. Zhang, E., Ren, J., Li, S., Yang, L., Qin, G., "Optimization of mechanical properties, biocorrosion properties and antibacterial properties of as-cast Ti–Cu alloys", ***Biomedical Materials***, Vol. 11, No. 6, (2016), 065001. https://doi.org/10.1088/1748-6041/11/6/065001
3. Zhang, E., Liu, C., "Effect of surface treatments on the surface morphology, corrosion property, and antibacterial property of Ti–10Cu sintered alloy", ***Biomedical Materials***, Vol. 10, No. 4, (2015), 045009. https://doi.org/10.1088/1748-6041/10/4/045009
4. Ohkubo, C., Shimura, I., Aoki, T., Hanatani, S., Hosoi, T., Hattori, M., Oda, Y., Okabe, T., "Wear resistance of experimental Ti–Cu alloys", ***Biomaterials***, Vol. 24, No. 20, (2003), 3377-3381. https://doi.org/10.1016/S0142-9612(03)00157-1
5. Akbarpour, M. R., Javadhesari, S. M., "Wear performance of novel nanostructured Ti-Cu intermetallic alloy as a potential material for biomedical applications", ***Journal of Alloys and Compounds***, Vol. 699, (2017), 882-886. https://doi.org/10.1016/j.jallcom.2017.01.020
6. Javadhesari, S. M., Alipour, S., Akbarpour, M. R., "Biocompatibility, osseointegration, antibacterial and mechanical properties of nanocrystalline Ti-Cu alloy as a new orthopedic material", ***Colloids and Surfaces B: Biointerfaces***, Vol. 189, (2020), 10889. https://doi.org/10.1016/j.colsurfb.2020.110889
7. Liu, J., Zhang, X., Wang, H., Li, F., Li, M., Yang, K., Zhang, E., "The antibacterial properties and biocompatibility of a Ti–Cu sintered alloy for biomedical application", ***Biomedical Materials***, Vol. 9, No. 2, (2014), 025013. https://doi.org/10.1088/1748-6041/9/2/025013
8. Javadhesari, S. M., Alipour, S., Akbarpour, M. R., "Effects of SiC nanoparticles on synthesis and antimicrobial activity of TiCu nanocrystalline powder", ***Ceramics International***, Vol. 46, No. 1, (2020), 114-120. https://doi.org/10.1016/j.ceramint.2019.08.240
9. Javadhesari, S. M., Alipour, S., Akbarpour, M. R., "Microstructural characterization and enhanced hardness, wear and antibacterial properties of a powder metallurgy SiC/Ti-Cu nanocomposite as a potential material for biomedical applications", ***Ceramics International***, Vol. 45, No. 8, (2019), 10603-10611. https://doi.org/10.1016/j.ceramint.2019.02.127
10. Han, Y., Wang, H. R., Cao, Y. D., Hou, W. T., Li, S. J., "Improved corrosion resistance of selective laser melted Ti–5Cu alloy using atomized Ti–5Cu powder", ***Acta Metallurgica Sinica (English Letters)***, Vol. 32, (2019), 1007-1014. https://doi.org/10.1007/s40195-019-00896-1
11. Zong, W., Zhang, S., Zhang, C., Ren, L., Wang, Q., "Design and characterization of selective laser-melted Ti6Al4V–5Cu alloy for dental implants", ***Materials and Corrosion***, Vol. 71, No. 10, (2020), 1697-1710. https://doi.org/10.1002/maco.202011650
12. Shon, I. J., Kim, N. R., Du, S. L., Ko, I. Y., Cho, S. W., Kim, W., "Rapid consolidation of nanostructured TiCu compound by high frequency induction heating and its mechanical properties", ***Materials Transactions***, Vol. 51, No. 11, (2010), 2129-2131. https://doi.org/10.2320/matertrans.M2010251
13. Akbarpour, M. R., Hesari, F. A., "Characterization and hardness of TiCu–Ti_2Cu_3 intermetallic material fabricated by mechanical alloying and subsequent annealing", ***Materials Research Express***, Vol. 3, No. 4, (2016), 045004. https://iopscience.iop.org/article/10.1088/2053-1591/3/4/045004
14. Hesabi, Z. R., Hafizpour, H. R., Simchi, A., "An investigation on the compressibility of aluminum/nano-alumina composite powder prepared by blending and mechanical milling", ***Materials Science and Engineering: A***, Vol. 454, (2007), 89-98. https://doi.org/10.1016/j.msea.2006.11.129
15. Nazari, K. A., Nouri, A., Hilditch, T., "Compressibility of a Ti-based alloy with varying amounts of surfactant prepared by high-energy ball milling", ***Powder Technology***, Vol. 279, (2015), 33-41. https://doi.org/10.1016/j.powtec.2015.03.044
16. Sivasankaran, S., Sivaprasad, K., Narayanasamy, R., Iyer, V. K., "An investigation on flowability and compressibility of AA 6061_{100-x}x wt.% TiO_2 micro and nanocomposite powder prepared by blending and mechanical alloying", ***Powder Technology***, Vol. 20, No. 1, (2010), 70-82. https://doi.org/10.1016/j.powtec.2010.03.013
17. Ramírez-Vinasco, D., León-Patiño, C. A., Aguilar-Reyes, E. A., Rodríguez-Ortiz, G., "Compressibility behaviour of conventional AlN-Cu mixtures and Cu-(AlN-Cu) composite powder mixtures", ***Powder Technology***, Vol. 403, (2022), 117385. https://doi.org/10.1016/j.powtec.2022.117385